

A Critical Review and Discussion of Different Methods to Determine the Series Resistance of Solar Cells: $R_{s,\text{dark}}$ vs. $R_{s,\text{light}}$?

Jan-Martin Wagner^{1, a)}, Koundinya Upadhyayula¹, Jürgen Carstensen¹,
and Rainer Adelung¹

¹*Christian-Albrechts-Universität zu Kiel, Technische Fakultät, Kaiserstraße 2, 24143 Kiel, Germany*

^{a)}Corresponding author: jwa@tf.uni-kiel.de

Abstract. Luminescence imaging, both in electroluminescence and photoluminescence mode, is employed to test the widely accepted notion that the lumped series resistance, R_s , measured in the dark, $R_{s,\text{dark}}$, differs from its value measured under illumination, $R_{s,\text{light}}$. Using the illumination intensity variation method to determine the series resistance allows us to treat measurements in the dark and under illumination on equal footing. We find (i) the already-known variation of R_s along the current–voltage characteristic in dependence on the total dark current I_D and (ii) that for standard operation conditions there is no difference between $R_{s,\text{dark}}$ and $R_{s,\text{light}}$ but only for external currents I_{ext} exceeding the 1-sun photocurrent. Previously reported differences are traced back to systematic errors in the R_s evaluation schemes used in those works.

INTRODUCTION

The standard way to model a solar cell’s internal series resistance is to represent all its series resistance effects (lateral voltage drop, Joule power loss) by a single ohmic resistor in the standard equivalent circuit. However, this is an oversimplification, because there are two experimental observations that are not covered by this model: (i) For large-area silicon solar cells this lumped R_s isn’t constant but varies along the current–voltage (I – U) characteristic. This is so because the relative importance of the lateral current flow in the emitter compared to the current flow through the base changes in dependence on the amount of the total forward-bias diode current I_D (also known, for short, as dark current). As a result, R_s becomes smaller in forward direction, most noticeably for voltages larger than U_{MPP} . Since this effect depends just on I_D , it occurs both in the dark and under illumination. Although it was described in the literature quite early [1] (and also found in more recent experimental works, *e.g.* [2–10]), it is often ignored (or wrongly taken as occurring just in the dark [11]). (ii) In several works different R_s values in the dark and under illumination are reported, with $R_{s,\text{dark}}$ being smaller than $R_{s,\text{light}}$ (*cf.*, *e.g.*, [3, 11, 12]). This cannot be understood on the basis of the equivalent circuit, since there the current flow direction doesn’t make any difference for R_s . Usually, such R_s differences are explained by current flow patterns in the bulk of the solar cell differing in the dark and under illumination [3, 13].

Obviously, from (i) and (ii) some questions arise, and in our contribution we are going to discuss at least the following ones: How can one measure the lumped R_s in a way that the above-described effects (i) and (ii) can be clearly identified? Does the same reason lead to these two effects? What do these two effects mean for the standard equivalent circuit? The first of these questions will be answered in the following part of this work; the others are discussed based on our experimental results.

THEORY: LUMPED SERIES RESISTANCE OF A SOLAR CELL

Robust Definition of R_s

There are many different methods to determine a lumped R_s value, based on various measurement conditions and data evaluation schemes. Over the years, already several review articles have appeared on this topic, all covering a bunch of methods (cf., e.g. [11, 14–16]). Therefore, although it is clear that a solar cell shows series resistance effects and that they can be measured in a lumped manner, it seems far from clear what “the” lumped series resistance is. However, there is one R_s determination method that needs the least information about a solar cell as input: the illumination intensity variation method [1] (also known as double illumination or two/multiple light level method [6]); it is known to be quite robust and reliable [6, 11]. This method amounts to record I – U data for two (or more) different illumination levels and compare those data points for which the forward-bias diode current I_D is identical. For a single pair of data being related in this way (marked by indices 1 and 2, for the two light intensities used) one obtains the lumped series resistance (that belongs to the relevant I_D) as

$$R_s(I_D) = \frac{\Delta U_{\text{ext}}(I_D)}{\Delta I_{\text{ext}}(I_D)} = \left. \frac{U_{\text{ext},2} - U_{\text{ext},1}}{I_{\text{ext},2} - I_{\text{ext},1}} \right|_{I_{\text{D},2} = I_{\text{D},1} = I_D}. \quad (1)$$

By requiring to use a constant I_D , in this method shunt currents and the nonlinearity due to the forward-biased p-n junction fully cancel. It was shown that this cancellation is even independent of the functional form of the forward characteristic [8]. This is so because this method works on single points of the I – U characteristic, therefore the latter’s overall shape doesn’t matter.

Basic Properties of R_s

The latter fact enables one to use an arbitrary I – U characteristic to illustrate and discuss this R_s determination method since, as just stated, the results do not depend on the characteristic but only on the forward-bias diode current I_D of the chosen data points. Here, we choose the simplest case of an I – U characteristic corresponding to the simplest standard equivalent circuit, without shunts and having only one diode, but we take into account the dependence of R_s on I_D ; this choice makes it is easy to obtain analytical results from which conclusions of general validity can be drawn:

$$I_{\text{ext}} = I_0 \left[\exp\left(\frac{U_{\text{ext}} - R_s(I_D)I_{\text{ext}}}{kT/q}\right) - 1 \right] - I_{\text{ph}} =: I_D - I_{\text{ph}} \quad (2)$$

Solving Eq. (2) for U_{ext} one obtains

$$U_{\text{ext}} = R_s(I_D)I_{\text{ext}} + U_{\text{th}} \ln\left(\frac{I_{\text{ext}} + I_{\text{ph}}}{I_0} + 1\right) = R_s(I_D)I_{\text{ext}} + \frac{kT}{q} \ln\left(\frac{I_D}{I_0} + 1\right) \quad (3)$$

As one can see from Eq. (3), the photocurrent doesn’t play any explicit role, so this approach is applicable to dark I – U data as well; then, $I_D = I_{\text{ext}}$, of course. Therefore, here the illumination variation method is taken as reference since it is universally applicable (*i.e.*, both in the dark and under illumination) and provides R_s in dependence on I_D .

Based on this method, it is easy to systematically check for a possible difference between $R_{s,\text{dark}}$ and $R_{s,\text{light}}$: Using the open circuit point (for which R_s is irrelevant) at a chosen illumination intensity as first data point in Eq. (1), one can obtain $R_{s,\text{dark}}$ by using as second data point the corresponding one on the dark I – U curve (*i.e.*, where $I_{\text{ext}} = I_D = I_{\text{ph},1}$), and $R_{s,\text{light}}$ by doubling the illumination intensity and taking as second data point the corresponding one where $I_{\text{ext}} = -I_{\text{ph},1}$, thereby inverting the external current flow compared to the dark case but keeping the overall injection level. Repeating this for different illumination intensities provides the dependences of $R_{s,\text{dark}}$ and $R_{s,\text{light}}$ on I_D , if present. However, to understand the basic qualitative behavior, it turns out that it is sufficient to consider just two different dark currents, one being equal to approximately the full 1 sun photocurrent, the other to about 1.5 times this current; the corresponding results are given in the following part of this work.

EXPERIMENT: LUMINESCENCE IMAGING

Approach: Local Voltage Determination from Luminescence Images

In general, as we have shown previously [9] (and references therein), when using measurements based on luminescence imaging, it is not only straightforward to find operating conditions in accordance with the illumination intensity variation method to determine the lumped R_s , but it is also simple to obtain a meaningful local series resistance image of the whole cell, with the arithmetic average of this image being equal to the relevant lumped R_s value. However, this method is based on a linear-response description of the solar cell (therefore it is abbreviated as LR- R_s method), and in the underlying theory there is no possibility for the lumped series resistance to differ between the dark case [measured by electroluminescence (EL)] and the illuminated case [measured by photoluminescence (PL) under current extraction]. Therefore, in order to test for a possible difference between $R_{s,dark}$ and $R_{s,light}$, we cannot use our standard LR- R_s method.

However, since the information gained from such EL and PL luminescence images relevant for the local series resistance determination comes from the local voltage, and since here in this work we are interested only in a comparison of the qualitative behavior of the series resistance for current entering or leaving the solar cell, it suffices to obtain images of the lateral voltage distribution corresponding to these cases. As was discussed *e.g.* in [17, 18], such local voltage images can be obtained from the local luminescence intensity in a more or less straightforward manner. Taking the relevant luminescence images according to the conditions of the illumination intensity variation method allows interpreting them according to the related R_s information. Moreover, since the conversion of local luminescence intensities to local voltages is free from the restrictions that apply to our LR- R_s method, it can be used also in cases where $R_{s,dark}$ and $R_{s,light}$ differ. That way, combining the voltage interpretation of luminescence images with the series information related to the illumination intensity variation method, we are able to draw relevant conclusions about a possible difference between $R_{s,dark}$ and $R_{s,light}$.

The main equation needed for the conversion of a luminescence image into a voltage image is based on the fact that the local luminescence intensity can be described as (*cf., e.g.*, [19, 20] and references therein)

$$\Phi(x,y) = C(x,y) \exp[U(x,y)/U_{\text{thermal}}], \quad (4)$$

with the thermal voltage $U_{\text{thermal}} = k_B T/e$. According to the conditions of the illumination intensity variation method, we take an EL image, an open-circuit image, and a PL image under current extraction, all with the same dark current I_D involved (as discussed above). Since the total luminescence intensity is proportional to the total dark current, the corresponding working points can be found directly from the luminescence images (simply by looking at their mean values). Then, taking the ratio between the EL (or the PL) image with the corresponding open-circuit image (*i.e.* calculating the ratio of the luminescence intensities pixel by pixel), the pre-factor $C(x,y)$ in Eq. (4) cancels, and taking the logarithm of this ratio, the corresponding voltage distribution is obtained (as difference to the voltage under open-circuit condition, which to a good approximation is laterally constant):

$$U_{\text{EL or PL}}(x,y) - U_{\text{oc}} = U_{\text{thermal}} \ln[\Phi_{\text{EL or PL}}(x,y)/\Phi_{\text{oc}}(x,y)]. \quad (5)$$

The important point here is that the lateral variation in the resulting voltage image mainly comes from the external current passing the series resistance network of emitter and grid on the front side of the solar cell. Therefore, comparing such voltage images for current flowing into the solar cell with those for current flowing out of it allows to qualitatively compare the effect of $R_{s,dark}$ and $R_{s,light}$. Further, it is clear from Eq. (5) that the main qualitative information about the current-flow-related voltage distribution comes from the ratio of the luminescence images and taking the logarithm of that ratio; this is what our experimental work is based on.

Due to the diffusion-limited carriers contributing to the PL intensity without being related to the local voltage [17, 21], in the literature one usually finds a different treatment for EL and PL images in the luminescence-based voltage determination. Yet this correction of the PL images is only needed when infrared light is used for illumination, because it has a large penetration depth, thereby leading to the creation of a significant amount of diffusion-limited carriers. In our experiments, however, we use red light for illumination, which has a very short penetration depth; it creates a minority carrier profile in the base not very different from the one in the EL case. Thus, only a negligible amount of diffusion-limited carriers is created. We have checked this by measuring PL images at short-circuit condition; those images essentially show just noise.

Results: Lateral Voltage Distribution in Dependence on I_D

Normal Operation Range of a Solar Cell: $I_D = |I_{ext}| = |I_{photo}|$

We start with measurements where we stay in the normal operation range of a solar cell, employing as external current value the absolute value of the photocurrent of the cell under investigation; in our case this are about 5 A.

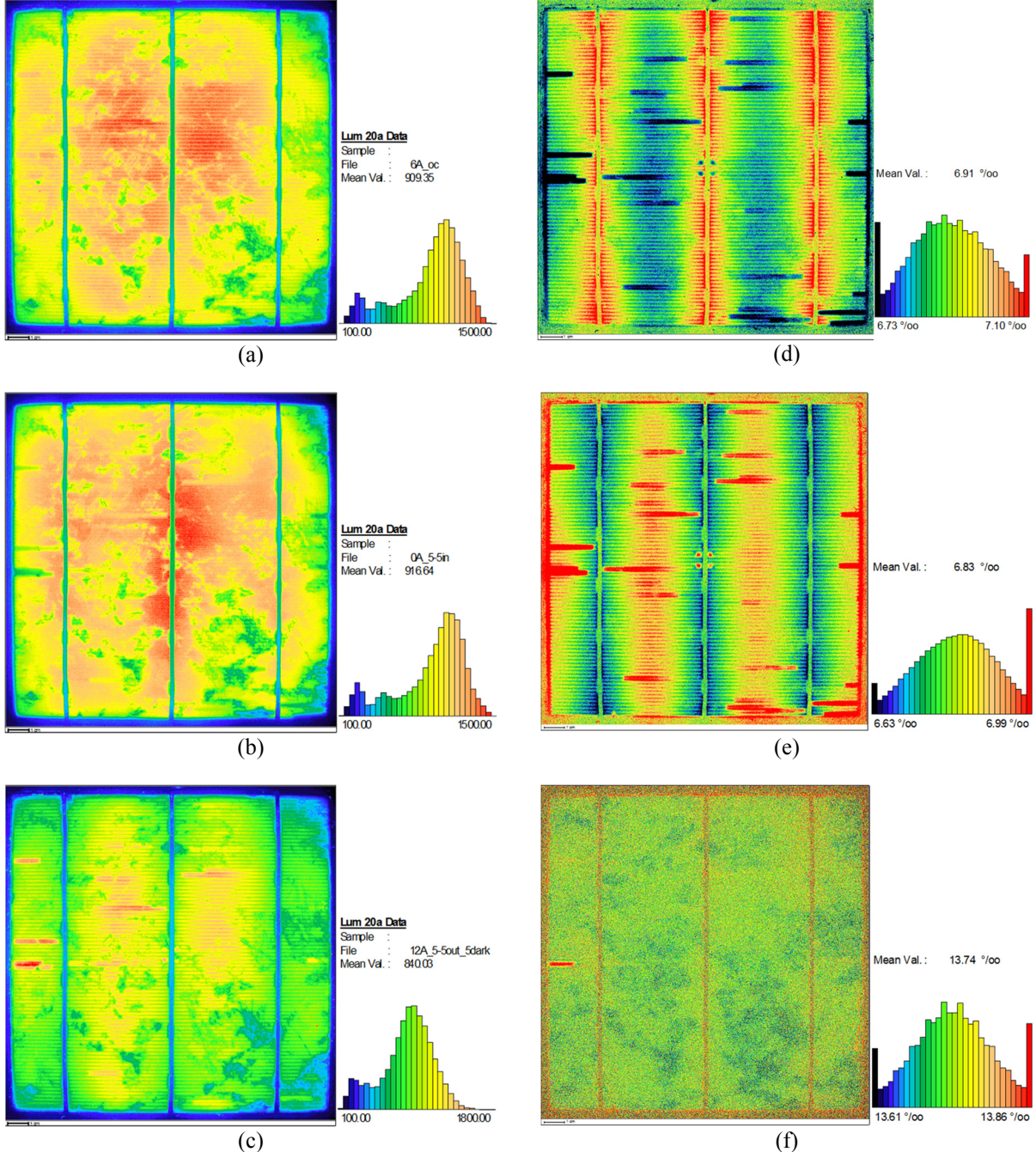


FIGURE 1. (a)–(c) Luminescence images of a solar cell at an injection of $I_D = I_{ph}(1 \text{ sun}) = 5 \text{ A}$: (a) open circuit, (b) EL, (c) PL with current extraction ($I_{ext} = 5 \text{ A}$). (d), (e) Voltage distribution according to Eq. (5) but in relative values only (without the prefactor U_{thermal}): (d) for EL, (e) for PL. (f) Sum of (d) and (e), showing no series resistance features; see text for details.

As described above, the first image is the one sun open circuit image where the whole one sun photocurrent flows as dark current I_D , leading to a certain injection on the solar cell [Fig. 1(a)]. The corresponding EL image is obtained by feeding an external current of 5 A into the solar cell so that the injection is the same as under open circuit [Fig. 1(b)]. To obtain the corresponding PL image, an illumination of 2 suns is needed, because then both the injection and the external current are each equal to the photocurrent [Fig. 1(c)]. Calculating the ratios of EL or PL and open circuit image and taking the logarithm gives the images shown in Fig. 1(d,e). As discussed above, they are proportional to the voltage distribution associated with the external current flow. As seen by naked eye, they seem to complement each other, *i.e.* that the voltage distribution for current flowing in appears to be the same as for the same current going out, just with the sign reversed. That this is indeed the case can be seen in Fig. 1(f), showing the sum of Fig. 1(d) and (e). Here, only contrast due to the low-lifetime areas occurs, but no series resistance features are seen, except for the pronounced deviation at the position where two neighboring grid fingers are broken.

$$\text{Beyond the Normal Operation Range of a Solar Cell: } I_D = |I_{\text{ext}}| = 1.5 |I_{\text{photo}}|$$

Using a larger current of 1.5 times the 1-sun photocurrent, in the following we go beyond the normal operation range of a solar cell; in our case this amounts to about 7.5 A. We are limited to this value because to obtain the relevant PL image, we used the maximum illumination available in our set-up, which are 3 suns; then, both the injection and the external current are each equal to 1.5 times the 1-sun photocurrent.

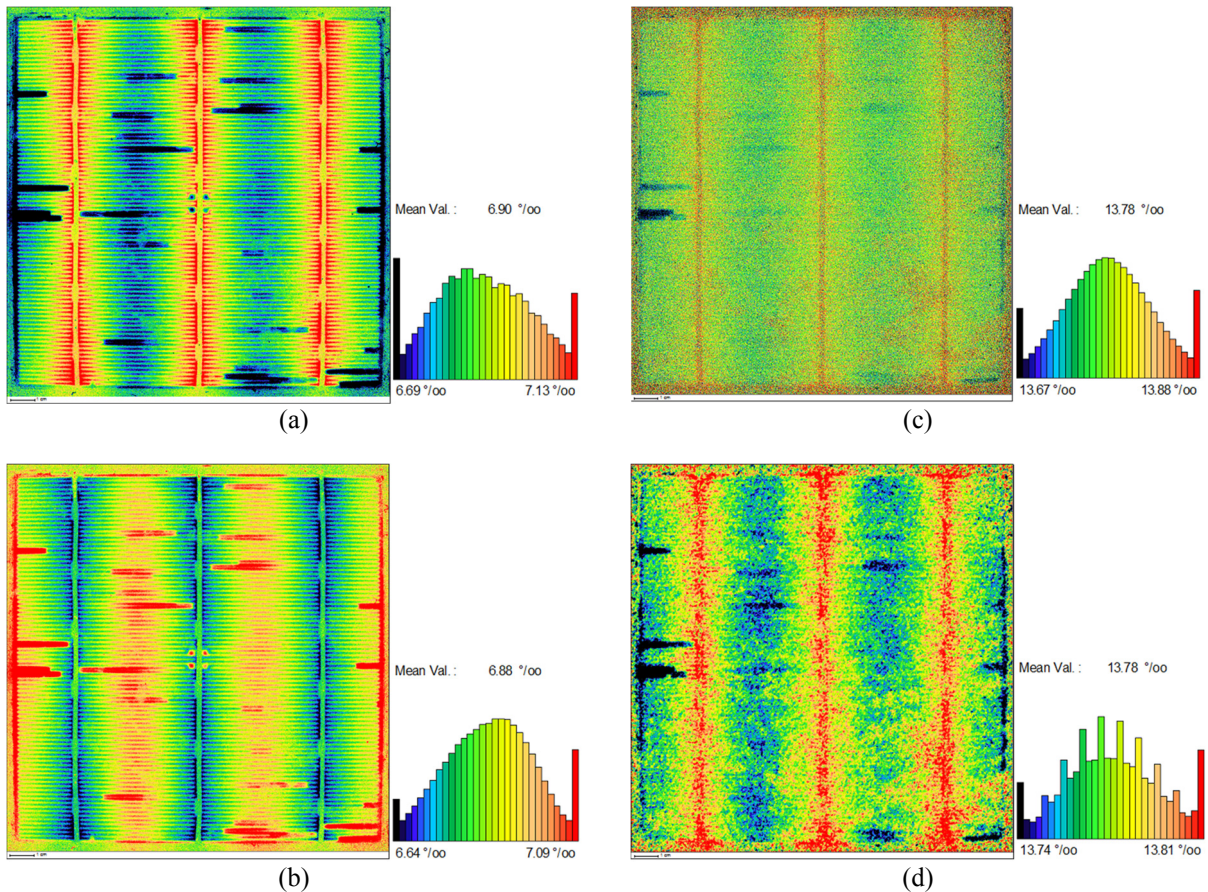


FIGURE 2. (a), (b) Voltage distribution according to Eq. (5) but in relative values only (without the prefactor U_{thermal}) of the same solar cell as in Fig. 1 but at an injection of $I_D = 1.5 I_{\text{ph}}(1 \text{ sun}) = 7.5 \text{ A}$: (a) for EL, (b) for PL with current extraction ($I_{\text{ext}} = 7.5 \text{ A}$). (c) Sum of (a) and (b), showing series resistance features similar to (a). (d) Same as (c) but slightly smoothed.

Since the directly measured luminescence images look similar to those in Fig. 1(a)–(c), they are not shown in Fig. 2. Calculating again the ratios between EL or PL and open circuit image and taking the logarithm gives the images

shown in Fig. 2(a,b). Also here they seem to complement each other. However, as Fig. 2(c) shows, in this case the sum of the voltage distributions for current flowing into and out of the solar cell does not even out, but many series resistance features can be seen. These features are emphasized by smoothing the image, as shown in Fig. 2(d): broken grid fingers and systematically higher values alongside the busbars, similar to Fig. 2(a). These findings are qualitatively different from the corresponding ones for lower current, Fig. 1(f).

Conclusions from the Experiments

As can be seen from Fig. 1(f), in the normal operation range, a current flowing into the solar cell or flowing out of it creates the same voltage distribution, just with the sign reversed. This means that the series resistance is independent of the current flow direction, *i.e.* there is no difference between $R_{s,\text{dark}}$ and $R_{s,\text{light}}$. This is consistent with our previous investigations where we explicitly derived the series resistance from the luminescence measurements; also there we didn't find a difference between $R_{s,\text{dark}}$ and $R_{s,\text{light}}$, just a dependence on I_D [9]. This is the behavior expected from our LR- R_s theory.

However, when going beyond the normal operation range, the series resistance features showing up in Fig. 2(c,d) indicate that there is a difference in the voltage distribution between inflow and outflow of current (of the same strength). This means that here we have an indication for a difference between $R_{s,\text{dark}}$ and $R_{s,\text{light}}$ being present. Since this is an effect beyond our LR- R_s theory, this points to the presence of large-scale inhomogeneities in the forward-bias diode current, leading to nonlinearities invalidating the approximation underlying Eq. (1) to describe the whole solar cell by a single value of the total forward-bias diode current. The latter only holds when the nonlinearity due to the forward-bias diode current is effectively cancelled, so that the linear behavior of the series resistance remains.

This interpretation (presence of nonlinearities for external currents beyond the normal operation range) is consistent with the fact that, when such a difference between $R_{s,\text{dark}}$ and $R_{s,\text{light}}$ is present, the equivalent circuit doesn't hold anymore. This is so because according to the equivalent circuit, also if modified to account for $R_s(I_D)$ [9], there is no (fundamental) difference with respect to R_s between the dark and the illuminated case (*i.e.* for current flowing into or out of the solar cell). The validity of the equivalent circuit, however, comes from the linearity of both the photocurrent (as described by the diffusion equation) and the voltage losses (as described by Ohm's law and the Poisson equation). That the series resistance indeed behaves linearly can be inferred from the experimental observation made for "properly designed" (also known as "economically feasible") solar cells that R_s just leads to voltage loss but not to current loss [22] – at least as long as the external current is not too high.

This allows to gain a deeper information from having a detailed look at Fig. 1(f): The most prominent feature appearing in this image, indicating that inward and outward current flow are not symmetric, is the position where two neighboring grid fingers are broken (about at the center of the left edge; appearing in red). There, the solar cell behaves nonlinearly, because locally the current is much larger than the grid was designed for. In contrast, single broken gridfingers can be bypassed without significant performance loss; they do not show up in Fig. 1(f).

To summarize, we have found that under normal operation conditions (*i.e.*, up to and around the maximum power point) there is no difference between $R_{s,\text{dark}}$ and $R_{s,\text{light}}$. Therefore, one can obtain the voltage and current distribution under illumination from that in the dark (and vice versa) just from a change in sign, an offset (to account for the different injection level as given by I_D) and a scaling factor (to account for different external current strengths).

DISCUSSION: OTHER METHODS TO DETERMINE SERIES RESISTANCE

The experimental observations and conclusions discussed above immediately lead to the question about the possible reasons for the observations reported in the literature (as mentioned in the introduction) about a systematic difference between $R_{s,\text{dark}}$ and $R_{s,\text{light}}$. Obviously, this contradicts our finding that such a difference is not present under normal operation conditions. However, as we have seen in the analysis of the present experiments, in order to draw meaningful conclusions about the series resistance behavior one has to apply a series resistance determination method that fully accounts for the dependence of R_s on the dark current I_D (as the illumination intensity variation method). If this is not properly taken into account, systematic errors may lead to wrong results and/or conclusions. Therefore, we check the methods used in Ref. [11] in that respect; and we find this problem to be present.

In the following, we refer to these methods by a separate mentioning of the type of R_s that they are designed for, because under normal operation conditions there is no difference between the series resistance in the dark and under illumination. So, basically all these methods just determine R_s .

Standard Curve Fit to Determine R_s (via $R_{s,\text{dark}}$)

A standard way to determine $R_{s,\text{dark}}$ is to use an analytical model that corresponds to the standard equivalent circuit, containing a globally fixed lumped R_s parameter (*i.e.*, there is no dependence on I_D), and to fit this expression to $I-U$ data measured in the dark, preferably to the high-current part (as in [11]) where the series resistance has the largest effect so it can be determined more reliably. However, since in this range R_s gets smaller for increasing $I_D = I_{\text{ext}}$, this method is prone to deliver an R_s value that (a) is seemingly smaller than determined by other methods where that part of the $I-U$ characteristic is not involved (so possibly giving rise to the misleading conclusion that $R_{s,\text{dark}} < R_{s,\text{light}}$ [11]) and that (b) is even not well-defined since it may depend on the voltage/current range used for fitting. (Analogous problems may occur when fitting an illuminated $I-U$ characteristic in a similar manner.)

Usage of the Dark Curve and Open Circuit Voltages to Determine R_s (via $R_{s,\text{dark}}$)

As already discussed in the experimental part above, this is just a special case of the illumination intensity variation method where the external current also determines the injection. It fully accounts for the dependence of R_s on I_D ; in exactly this way we have obtained our voltage distributions in the dark, using an EL and an open-circuit image. Originally, this method was already proposed by Rohatgi *et al.* [23], however without noting the possible dependence of R_s on I_D .

Usage of the One-Sun and the Dark Curve

Also this data combination can be handled directly by Eq. (1); it is just the special case where always $|I_{\text{ext},2} - I_{\text{ext},1}| = I_{\text{ph}}$ in the denominator. However, in the original literature R_s in this case is obtained from shifting the dark curve by $-I_{\text{ph}}$, taking the difference of the voltages at I_{MPP} and dividing by $|I_{\text{MPP}}|$ [3], thereby ending up with a slightly deviating value: Since $|I_{\text{MPP}}| < I_{\text{ph}}$, this results in an erroneously larger $R_{s,\text{light}}$ [3].

Usage of the One-Sun and the Dark Curve Including Dicker's Correction

In his dissertation of 2003 [24] Dicker proposes to correct the mismatch between voltage and current as just described by subtracting the part of the voltage that is due to the dark current flow as obtained from $R_{s,\text{dark}}$ times the dark current, $|I_{\text{ph}}| - |I_{\text{MPP}}|$. In principle, this can lead to the correct value of R_s , provided that $R_{s,\text{dark}}$ has been determined correctly (which, as discussed above, is not always the case, however).

IEC 60891 Standard for R_s Determination (via $R_{s,\text{light}}$)

The IEC standard 60891 [25] is based on the illumination intensity variation method; however, it refers to the maximum power point only and lacks the explicit statement that the such-determined lumped $R_{s,\text{light}}$ value is valid for correspondingly small I_D values only (where the variation of R_s vanishes because I_D is very low).

SUMMARY

In general, the most common problems involved in standard methods to determine the series resistance are that (1) values resulting from different methods are not compared on a physically sound basis, namely for identical forward-bias diode current I_D , possibly leading to wrong conclusions about differences between $R_{s,\text{dark}}$ and $R_{s,\text{light}}$; (2) methods seem to be restricted to the MPP but could provide reliable R_s data also for other operating points along the $I-U$ curve; (3) no warning is given about the variation of R_s along the $I-U$ curve, *i.e.* that the R_s value determined at a certain operating point (*e.g.*, at MPP) is indeed valid at this operating point (or, when determined at MPP, for lower voltages only, corresponding to small I_D values where the R_s variation can be neglected). One always has to bear in mind that (a) the variation of R_s comes from the forward-bias diode current I_D only (and *not* the external current), but (b) that this $R_s(I_D)$ times the external current gives the actual voltage drop at R_s .

ACKNOWLEDGMENTS

J.-M. Wagner acknowledges technical support from the Chair for Functional Nanomaterials (Prof. R. Adelung) and the Chair for Multicomponent Materials (Prof. F. Faupel), Technical Faculty at the University of Kiel.

REFERENCES

1. M. Wolf and H. Rauschenbach, *Advanced Energy Conversion* **3**, 455–479 (1963).
2. D. K. Bhattacharya, A. Mansingh, and P. Swarup, *Solar Cells* **18**, 153–162 (1986).
3. A. G. Aberle, S. R. Wenham, and M. A. Green, “A new method for accurate measurements of the lumped series resistance of solar cells,” in *Conference Record of the 23rd IEEE Photovoltaic Specialists Conference (Louisville, Kentucky, USA, 1993)*, edited by N. N. (IEEE, New York, 1993), pp 133–139.
4. S. Bowden and A. Rohatgi, “Rapid and accurate determination of series resistance and fill factor losses in industrial silicon solar cells,” in *Proceedings of the 17th European Photovoltaic Solar Energy Conference (Munich, Germany, 2001)*, pp. 1802–1805.
5. J. Carstensen, A. Abdollahinia, A. Schütt, and H. Föll, “Characterization of the grid design by fitting of the distributed serial grid resistance to CELLO resistance maps and global IV curves,” in *Proceedings of the 24th European Photovoltaic Solar Energy Conference (Hamburg, Germany, 2009)*, pp. 516–519.
6. K. C. Fong, K. R. McIntosh, and A. W. Blakers, *Progress in Photovoltaics: Research and Applications* **21**, 490–499 (2013).
7. O. Breitenstein and S. Rißland, *Solar Energy Materials & Solar Cells* **110**, 77–86 (2013).
8. M. Turek, *Journal of Applied Physics* **115**, 144503 (2014).
9. J.-M. Wagner, A. Schütt, J. Carstensen, and R. Adelung, *Energy Procedia* **92**, 255–264 (2016).
10. J.-M. Wagner, S. Rißland, A. Schütt, J. Carstensen, and R. Adelung, *Energy Procedia* **124**, 197–206 (2017).
11. D. Pysch, A. Mette, and S. W. Glunz, *Solar Energy Materials & Solar Cells* **91**, 1698–1706 (2007).
12. A. Mette, D. Pysch, G. Emanuel, D. Erath, R. Preu, and S. W. Glunz, *Progress in Photovoltaics: Research and Applications* **15**, 493–505 (2007).
13. P. P. Altermatt, G. Heiser, A. G. Aberle, A. Wang, J. Zhao, S. J. Robinson, S. Bowden, and M. A. Green, *Progress in Photovoltaics: Research and Applications* **4**, 399–414 (1996).
14. M. Bashahu and A. Habyarimana, *Renewable Energy* **6**, 129–138 (1995).
15. D. T. Cotfas, P. A. Cotfas, and S. Kaplanis, *Renewable and Sustainable Energy Reviews* **28**, 588–596 (2013).
16. G. M. M. W. Bissels, J. J. Schermer, M. A. H. Asselbergs, E. J. Haverkamp, P. Mulder, G. J. Bauhuis, and E. Vlieg, *Solar Energy Materials & Solar Cells* **130**, 605–614 (2014).
17. M. Glatthaar, J. Haunschild, R. Zeidler, M. Demant, J. Greulich, B. Michl, W. Warta, S. Rein, and R. Preu, *Journal of Applied Physics* **108**, 014501 (2010).
18. M. Kasemann, L. M. Reindl, B. Michl, W. Warta, A. Schütt, and J. Carstensen, *IEEE Journal of Photovoltaics* **2**, 181–183 (2012).
19. U. Rau, *Physical Review B* **76**, 085303 (2007).
20. K. Bothe and D. Hinken, “Quantitative Luminescence Characterization of Crystalline Silicon Solar Cells,” in *Semiconductors and Semimetals, Vol. 89: Advances in Photovoltaics, Part 2*, edited by G. P. Willeke and E. R. Weber (Academic Press, Burlington, 2013), pp. 259–339.
21. M. Kasemann, D. Grote, B. Walter, W. Kwapisil, T. Trupke, Y. Augarten, R. A. Bardos, E. Pink, M. D. Abbott, and W. Warta, *Progress in Photovoltaics: Research and Applications* **16**, 297–305 (2008).
22. K. B. Böer, R. M. Swanson, and R. A. Sinton, in *Advances in Solar Energy*, vol. 6 (Plenum Press, New York, 1990), p. 438.
23. A. Rohatgi, J. R. Davis, R. H. Hopkins, P. Rai-Choudhury, P. G. McMullin, and J. R. McCormick, *Solid-State Electronics* **23**, 415–422 (1980).
24. J. Dicker, “Analyse und Simulation von hocheffizienten Silizium-Solarzellenstrukturen für industrielle Fertigungstechniken,” Ph.D. thesis, University of Konstanz, Germany, 2003; pp. 129–143.
25. International Standard IEC 60891 (second edition), “Photovoltaic devices – Procedures for temperature and irradiance corrections to measured I-V characteristics,” section 5: “Determination of internal series resistance RS and R'S” (International Electrotechnical Commission, Geneva, 2009).